International Journal of Pharmaceutics 548 (2018) 759–770

Contents lists available at ScienceDirect

International Journal of Pharmaceutics

journal homepage: www.elsevier.com/locate/ijpharm

E-selectin targeted immunoliposomes for rapamycin delivery to activated endothelial cells

Shima Gholizadeh[a], Ganesh Ram R. Visweswaran[b], Gert Storm[a], Wim E. Hennink[a], Jan A.A.M. Kamps[b], Robbert J. Kok[a,*]

[a] Department of Pharmaceutics, Utrecht Institute for Pharmaceutical Sciences, Utrecht University, Utrecht, The Netherlands
[b] Department of Pathology & Medical Biology, Medical Biology Section, University Medical Center Groningen, University of Groningen, Groningen, The Netherlands

ARTICLE INFO

Keywords:
Immunoliposomes
Rapamycin
Targeted delivery
Endothelial cells

ABSTRACT

Activated endothelial cells play a pivotal role in the pathology of inflammatory disorders and thus present a target for therapeutic intervention by drugs that intervene in inflammatory signaling cascades, such as rapamycin (mammalian target of rapamycin (mTOR) inhibitor). In this study we developed anti-E-selectin immunoliposomes for targeted delivery to E-selectin over-expressing tumor necrosis factor-α (TNF-α) activated endothelial cells. Liposomes composed of 1,2-dipalmitoyl-*sn-glycero*-3.;hosphocholine (DPPC), Cholesterol, and 1,2-Distearoyl-*sn-glycero*-3-phosphoethanolamine-N-[methoxy(polyethyleneglycol)-2000]-maleimide (DSPE-PEG-Mal) were loaded with rapamycin via lipid film hydration, after which they were further functionalized by coupling N-succinimidyl-S-acetylthioacetate (SATA)-modified mouse anti human E-selectin antibodies to the distal ends of the maleimidyl (Mal)-PEG groups. In cell binding assays, these immunoliposomes bound specifically to TNF-α activated endothelial cells. Upon internalization, rapamycin loaded immunoliposomes inhibited proliferation and migration of endothelial cells, as well as expression of inflammatory mediators. Our findings demonstrate that rapamycin-loaded immunoliposomes can specifically inhibit inflammatory responses in inflamed endothelial cells.

1. Introduction

The mammalian target of the drug rapamycin is a 289-kDa serine/threonine kinase, typically known as mammalian target of rapamycin (mTOR). This mTOR kinase is a component of two different cellular signaling regulating complexes, known as mTOR complex 1 and 2 (mTORc1 and mTORc2) (Kim et al., 2002; Jacinto et al., 2004; Sarbassov et al., 2004; Wullschleger et al., 2006). The aforementioned proteins interact with specific downstream targets that are responsible for the interconnection of mTOR to different downstream signaling pathways such as Akt, SGK1 and 4E-BP1 that are involved in a variety of cellular processes such as cell survival, proliferation and cytoskeletal organization. Recent studies have highlighted the pivotal role of the mTOR pathways in inflammatory disorders (Cejka et al., 2010; Xie et al., 2014; Weichhart et al., 2015; Li et al., 2016). Also, a significant effect of mTOR on the progression of chronic kidney disease (CKD) has recently been suggested in several preclinical studies (Lieberthal and Levine, 2009, 2012). Other preclinical studies using animal models (e.g. rat models of CKD) have shown that the inhibition of mTOR signaling pathways by rapamycin resulted in a significant reduction of the influx of inflammatory cell into the diseased area (Bonegio et al., 2005; Wu et al., 2006). The inhibition of mTOR signaling pathways by rapamycin was also shown to significantly reduce the release of pro-inflammatory and pro-fibrotic cytokines, as well as fibrotic tissue formation, thus improving overall kidney function (Bonegio et al., 2005; Wu et al., 2006).

Rapamycin is a macrolide compound with hydrophobic characteristics (Log P: 4.3) (Simamora and Yalkowsky, 2001) resulting in poor water solubility, slow dissolution rate and consequential low oral bioavailability (Simamora and Yalkowsky, 2001; Hu et al., 2012). Nanocarrier formulations can overcome the problems associated with the poor biopharmaceutical characteristics of rapamycin, and thus can contribute to an improved safety and efficacy profile (Woo et al., 2012; Chen et al., 2013; Shah et al., 2013). Several rapamycin formulations have been reported in literature, based on various types of nanocarrier systems such as polymeric blend nanoparticles composed of the diblock copolymer polyethylene glycol–poly-L-lactic acid (mPEG–PLA) mixed with acid-terminated PLA (Woo et al., 2012); micelles composed of mixed diblock copolymers mPEG-b-P(HPMA-Lac-co-His) and mPEG-b-PLA (Chen et al., 2013); and liposomes composed of soy

* Corresponding author at: Department of Pharmaceutics, Utrecht Institute for Pharmaceutical Sciences, Utrecht University, Utrecht, The Netherlands.
E-mail address: r.j.kok@uu.nl (R.J. Kok).

http://dx.doi.org/10.1016/j.ijpharm.2017.10.027
Received 12 April 2017; Received in revised form 25 September 2017; Accepted 11 October 2017
Available online 13 October 2017

phosphatidylcholine (SPC), cholesterol (Chol) and 1,2-distearoyl-sn-*glycero*-3-phosphoethanolamine-*N*-[amino(polyethyleneglycol)-2000] (DSPE-PEG) (Eloy JO, 2016).

While many of the current anti-inflammatory therapeutic approaches are focused on attempts to suppress the activity of immune effector cells, recently there has been a growing interest toward understanding the role of endothelial cells in leukocyte recruitment into inflamed tissues (Panés et al., 1999; Muller, 2003). Endothelial cells are in direct contact with the blood which makes these cells attractive targets for nanocarrier delivery strategies. Selective delivery to inflamed endothelial cells is possible by targeting adhesion molecules (e.g. E-selectin, P-selectin, intercellular adhesion molecule (ICAM) and vascular cell adhesion molecule-1 (VCAM-1)) on their surface. Adhesion molecules are selectively (over)expressed in the presence of inflammatory stimulants such as interleukin-1 (IL-1), lipopolysaccharides (LPS) and tumor necrosis factor-α (TNF-α) (Cook-Mills and Deem, 2005). Proper cell selective delivery of potent anti-inflammatory agents may provide an important tool to both increase the efficacy and reduce the side effects of such therapeutic compound (i.e. rapamycin) in the treatment of inflammatory disorders (Koning et al., 2006).

In this study, we have developed anti-E-selectin antibody (Ab) coupled immunoliposomes, loaded with rapamycin, for targeted delivery to TNF-α activated endothelial cells (Fig. 1). This work discusses the characterization and formulation of the immunoliposomes, while their cell binding and uptake properties by TNF-α activated endothelial cells are also investigated. To evaluate the pharmacologic effects of the rapamycin containing immunoliposomes, cell proliferation and motility, phosphorylation of mTOR kinases, and inflammatory gene expression levels were analyzed.

2. Materials and methods

2.1. Materials

1,2-Distearoyl-*sn-glycero*-3-phosphoethanolamine-N-[methoxy(polyethyleneglycol)-2000]-maleimide (Mal-PEG_{2000}-DSPE), 1,2-dipalmitoyl-*sn-glycero*-3-phosphocholine (DPPC) and 1,2-dimyristoyl-*sn-glycero*-3-phosphoethanolamine-N-(lissamine rhodamine B sulfonyl) (Rho-PE) were obtained from Avanti Polar Lipids (Alabaster AL, USA). Cholesterol (Chol) and N-succinimidyl-S-acetylthioacetate (SATA) were purchased from Sigma-Aldrich (St. Louis MO, USA).

Rapamycin (Sirolimus) was purchased from LC laboratories. 4′,6-Diamidino-2-phenylindole (DAPI) was obtained from Roche (Woerden, The Netherlands) and paraformaldehyde from Fluka (Zwijndrecht, The Netherlands). All chemicals used were of analytical grade unless otherwise stated.

2.2. Preparation of liposomes

Liposomes were prepared from a mixture of DPPC, Cholesterol and Mal-PEG_{2000}-DSPE in the respective molar ratio of 65: 25: 10 which equals to respective amounts of 43, 9 and 27 mg in 3 ml of chloroform: methanol (9:1, v/v) to a final concentration of 30 mM total lipid (TL). Fluorescently labeled liposomes were prepared by adding Rhodamine-PE to the lipid mixture at 0.2 mol% of total lipid. Rapamycin was dissolved with the lipid mixture at a concentration of 20 nmol/μmol TL, which is equivalent to 1.7 mg rapamycin. Organic solvents were removed using a rotary evaporator and subsequent drying under a nitrogen flow. The resulting drug-lipid film was hydrated by adding 3 ml of HBS buffer pH 7.4 (10 mM Hepes containing 135 mM NaCl), followed by sonication in an ice-bath using a tip sonicator (Bandelin Sonopuls) for 10 min and incubation for 1 h at room temperature. Unilamellar liposomes were prepared by multiple extrusion steps using a Lipex™ Extruder (Northern Lipids, Burnaby, BC, Canada) over polycarbonate membranes (Nuclepore, Pleasanton, CA, USA) at different pore size range (from 0.4 μm to 0.1 μm). PEGylated Liposomes (i.e. prepared with PEG_{2000}-DSPE instead of Mal-PEG2000-DSPE and without further E-Selectin addition, see below) are referred to as non-targeted or control liposomes. For preparation of targeted liposomes, liposomes were decorated with mouse anti-human E-selectin antibody H18/7 (IgG2a). The H18/7 antibody was produced in-house by hybridoma cell culture kindly provided by Dr. M. Gimbrone Jr. (Harvard

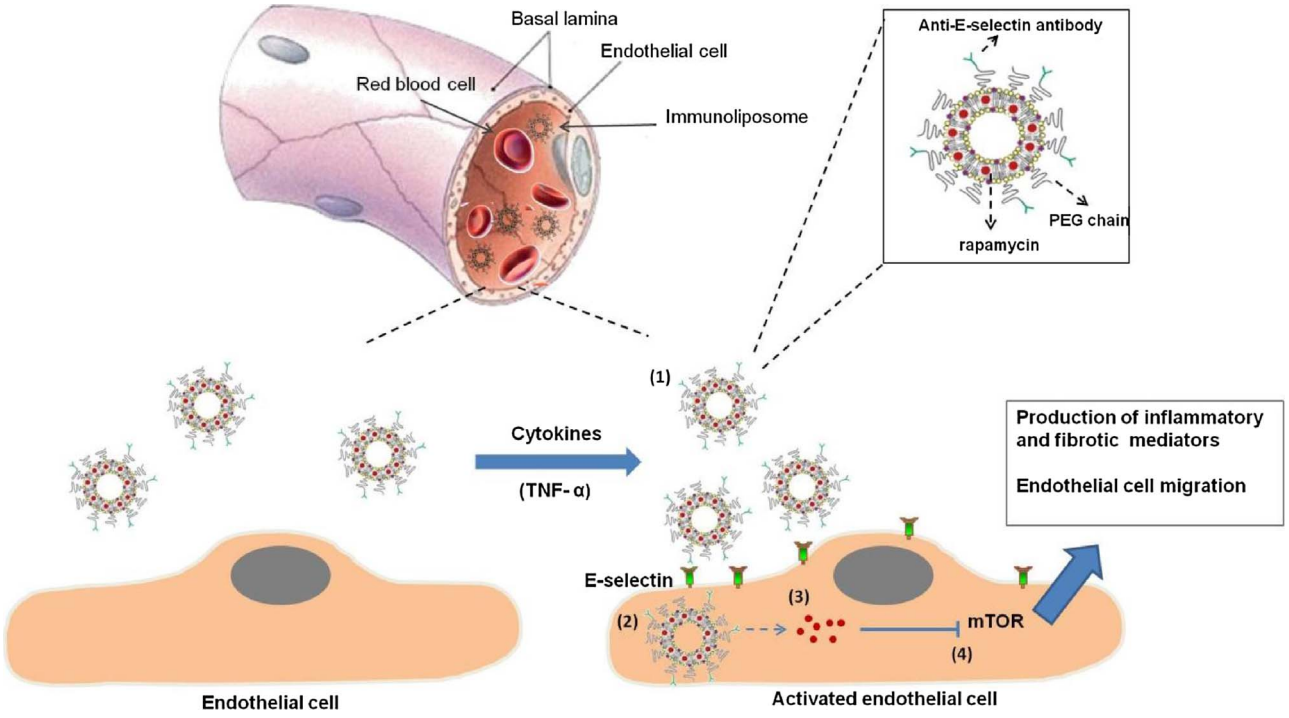

Fig. 1. Conceptof targeted delivery of rapamycin to TNF-α activated (i.e. inflamed) endothelial cells. Immunoliposomes decorated with anti-E-selectin antibodies **(1)** interact with E-selectin adhesion molecules expressed on the cell surface of TNF-α activated endothelial cells **(2)**. Receptor-mediated uptake and intracellular delivery/cytosolic release of rapamycin molecules **(3)** eventually lead to inhibition of mTOR pathway **(4)**. Adapted with permission from ref (Martini et al., 2012). Copyright 2012, Pearson education Inc.

Medical School, Boston, MA) and purified by protein-G affinity chromatography (protein G Sepharose fast flow) and dialysis against PBS as described previously (Everts et al., 2003). H18/7 was modified with S-acetylthioacetyl (SATA) (8:1 SATA:Ab mol:mol ratio). SATA-modified anti-human E-selectin antibody (2 mg/ml in HBS buffer) was treated with hydroxylamine 0.5 M for 45 min to deprotect the thioacetyl groups and subsequently reacted to the maleimidyl groups on the liposomes at 15 μg/μmol TL as described before (Everts et al., 2003). Non-reacted antibody and non-encapsulated rapamycin were removed by passing liposomes over a PD10 desalting column (GE Healthcare Life Sciences™) followed by ultrafiltration using Vivaspin centrifugal concentrators (Sartorius AG, Aubagne, France) with a molecular weight cut-off membrane of 300-kDa.

2.3. Characterization of liposomes

Liposome sizes and polydispersities were measured using dynamic light scattering (DLS) on an ALV CGS-3 system (Malvern Instruments, Malvern, UK). Zeta-(ζ) potential of liposomes was measured using a Malvern Zetasizer Nano-Z (Malvern Instruments, Malvern, UK) with universal ZEN 1002 dip cells and DTS (Nano) software. Rapamycin content of the liposomes was determined in 100 μl aliquots which were disrupted by diluting in 300 μl of acetonitrile. Rapamycin content was determined by high performance liquid chromatography on a Waters Acquity HPLC system (Waters Corporation, Milford, MA, USA) equipped with a Sunfire C18 column (5 μm bead size; 4.6 × 150 mm) thermostated at 60 °C and a UV detector operated at 290 nm. The isocratic mobile phase (1 ml/min) was composed of 70% acetonitrile and 30% water. For each sample batch, six calibration points were always prepared using serial dilutions of rapamycin in acetonitrile in the concentration range: 200, 160, 120, 80, 40nmol/ml and blanc matrix). Calibration samples with a concentration of 40 nmol/ml (i.e. lowest concentration in the calibration) could be easily measured on the HPLC system, achieving good signal to noise ratios (S/N > > 10). The total lipid concentration was determined according to Rouser et al. (Rouser et al., 1970). Conjugation of Ab to the surface of liposomes was confirmed with dot blot assay, using HRP conjugated Goat-anti-Mouse IgG (H + L) Secondary Antibody (Thermo Fischer Scientific). Liposomes were further characterized by determining the concentration of surface coupled Ab, using mouse IgG (Sigma Aldrich) as a standard via Micro-BCA assay (Pierce Biotechnology, Rockford, IL, USA).

The number of antibody molecules coupled per liposome (p) was calculated by geometric arguments according to formula (1) below, as described previously by Adrian and co-workers (Adrian et al., 2007).

$$p = \pi/6 \times C_{Ab} \times (3d_{bl} \times R^2 – 3R \times {d_{bl}}^2 + {d_{bl}}^3) \times {M_{ab}}^{-1} \times {V_{Ls}}^{-1} \quad (1)$$

In which (C_{Ab}) is measured concentration of antibody (gram per mol of lipid), (R) is the average diameter (nanometers) of the spherical liposomes, (V_{Ls}) and (d_{bl}) represent specific lipid volume and lipid bilayer thickness, respectively, and (M_{Ab}) is the molecular mass of the antibody.

2.4. Cell lines and culture conditions

Human umbilical vein endothelial cells (HUVEC) were obtained from Lonza (Breda, The Netherlands). Cells were grown in endothelial cell growth medium-2 (EGM-2) (Lonza, Breda, The Netherlands), consisting of endothelial basal medium-2 (EBM-2) supplemented with growth factors and antibiotics (EGM-2 SingleQuots kit, Lonza). The cells were kept in culture at 37 °C in a humidified atmosphere containing 5% CO_2/95% air. Experiments were performed with cells of passage 3–7.

2.5. Binding and uptake of fluorescent labeled liposomes

Binding of liposomes was studied by incubating TNF-α activated endothelial cells with rhodamine-labeled liposomes at 4 °C. HUVEC were seeded at 8000 cells/well in 6-well chamber slides (Lab-Tek® supplier). After 24 h, the cells were activated with TNF-α (recombinant human tumor necrosis factor-α; Boehringer, Mannheim, Germany), at concentration of 10 ng/ml for 4 h at 37 °C and subsequently incubated with rhodamine labeled liposomes at 4 °C (0.5 mM TL; 1 h at 4 °C). Cells were washed with PBS and fixed with 4% paraformaldehyde in PBS. Nuclei were stained with DAPI (1 μg/ml; 5 min at room temperature) and washed again with PBS. Slides were mounted on glass cover slide using fluorSave (Calbiochem, San Diego, CA, USA) and analyzed for binding of labeled liposomes with a Keyence microscope (BZ-9000 BioRevo, Keyence®).

Uptake of Rhodamine labeled liposomes by TNF-α activated endothelial cells was determined by flow cytometry. HUVEC were added at concentration of 10,000 cells/well in U-bottom shaped 96-well plates (Becton & Dickinson, Mountain View, CA, USA), activated with TNF-α (10 ng/ml; 4 h at 37 °C) and subsequent incubated with rhodamine labeled liposomes in a concentration range of 0.02–3 μM TL in EGM-2 cell culture medium for 3 h at 37 °C in the dark. After removal of culture medium and excess of liposomes the cells were washed three times with cold PBS containing 0.3% BSA. Cells were collected by centrifugation for 5 min at 500*g* at 20 °C and washed with an acidic buffer (200 mM glycine containing 150 mM NaCl, pH 3.0) to remove cell surface bound liposomes. Next, cells were fixed with 10% formalin solution. Uptake of Rhodamine labeled liposomes by the cells was quantified via flow cytometry with BD FACSCanto (Becton & Dickinson). Per sample 10,000 events were collected and the samples were prepared in triplicate. Data were analyzed with BD FACSDiva™ software (Becton & Dickinson) and expressed as mean fluorescence intensity.

2.6. Effects of rapamycin-loaded liposomes on cultured cells

2.6.1. Effect of rapamycin on cell viability

The cell viability upon incubation with rapamycin at different concentrations was evaluated via MTS assay, which measures the mitochondrial (metabolic) activity of the cells. HUVEC were seeded into 96-well plates: 8000 cells were seeded per well. After 24 h of seeding the medium was refreshed with fresh medium containing TNF-α (10 ng/ml), and 50 μl of rapamycin dilutions in medium prepared from a stock solution of rapamycin in DMSO was added to the cells, corresponding to a final concentration of 2.5–50 μM. After 48 h of incubation, MTS assay (Promega, Leiden, The Netherlands) was performed according to manufacturer's protocol.

2.6.2. Effect of rapamycin liposomes on migration of endothelial cells

HUVEC were seeded in 6 well plates at a density of 80,000 cells per well. After overnight adherence of the cells to the well plates in full EGM-2 medium, cells were activated with TNF-α (10 ng/ml; 4 h at 37 °C), followed by treatment with either free rapamycin or different liposomal formulations equivalent to 10 μM rapamycin. After 12 h, a scratch wound was made in the cell monolayer with a p20 pipet tip. Cells and dimensions of the scratch wound were imaged and recorded at 20 x magnification with a Nikon TE2000 microscope. Cells were washed once with PBS and incubated for an additional 16 h with fresh medium before imaging of the scratch wound areas. Scratch wound surface area was analyzed using NIH ImageJ software, and expressed relative to the initial scratch wound area.

2.6.3. Effect of rapamycin liposomes on proliferation of endothelial cells

The effect of rapamycin and liposomes containing rapamycin on endothelial cell proliferation was analyzed in two different

experimental setups, using either short-term exposure followed by a recovery period or long-term continuous exposure. In detail, HUVEC were seeded at a density of 5000 cells/well in 96-well plates. After overnight adherence to the plates, cells were activated with TNF-α as described above (10 ng/ml for 4 h at 37 °C) after which the medium was replaced by fresh culture medium containing either free rapamycin or liposomal rapamycin in a concentration range of 25 nM − 40 μM. For short term exposure, the medium was refreshed with drug-free medium after 4 h followed by an additional 44 h incubation period, while long-term exposure involved one continuous 48 h period of incubation with drug-containing medium. Next, culture media were replaced by drug-free medium containing BrdU reagent (Roche Applied Science, Penzberg, Germany), after which cells were cultured for an extra 24 h (in total 72 h). Cell proliferation was assayed by BrdU-colorimetric immunoassay according to the supplier's protocol. A standard curve was created in order to convert sample optical density (OD) values into proliferating cell numbers per well. Sequential dilutions of cells were prepared from a stock solution to obtain a calibration curve for the response of various concentrations of cells (781, 1563, 3125, 6250 and 125000 cells per well), as a double linear plot of absorbance values (OD) against proliferating cell number. Cells were seeded and cultured for 24 h. Cells were incubated with BrdU reagent for an extra 24 h and incorporation of BrdU was detected with a BrdU cell proliferation ELISA kit. The total number of cells required to construct the curve in triplicate was 2.4×10^6, which is a quantity that can be harvested from a 70% confluent T175 flask (175 cm^2).

2.6.4. Effect of rapamycin liposomes on mRNA expression and intracellular signaling

The effect of rapamycin liposomes on inflammatory signaling was investigated by Q-PCR mRNA expression analysis. HUVEC were seeded in 12 well plates at 50,000 cells per well and allowed to adhere overnight before activation with TNF-α for 4 h at 37 °C, followed by incubation for 24 h at 37 °C with medium containing either 10 μM rapamycin or its equivalent in liposomal rapamycin. RNA was isolated using RNeasy® Mini Plus Kits (Qiagen, Venlo, the Netherlands) according to the manufacturer's protocol. The concentration of RNA was determined by both NanoDrop® ND-1000 spectrophotometer (Wilmington, DE) and by agarose (1%) gel electrophoresis. Complementary DNA (cDNA) to respective RNA samples was generated by a 20 μl mixture containing SuperScript™ III RNaseH-Reverse Transcriptase (Invitrogen, supplied by Life Technologies, Bleiswijk, the Netherlands), RNaseOut inhibitor (40 U) (Invitrogen) and 250 ng random hexamers (Promega, Leiden, the Netherlands). cDNA solutions were diluted to 10 ng/ml with MilliQ, and 1 μl was used for each PCR reaction.

Human GAPDH (Hs99999905_m1), E-selectin (Hs00174057_m1), VCAM-1(Hs00365486_m1), VEGF-A (Hs00173626_m1), hTIE2 (Hs00176096_m1), TGF-b (Hs00171257_m1) and mTOR (Hs01042424_m1) primer probes were purchased as Assay-on-Demand from Applied Biosystems (Nieuwerkerk a/d IJssel, the Netherlands). These primer probes together with Absolute QPCR Rox Mix (Thermo Fischer Scientific) were used for real-time PCR analysis performed on an ABI PRISM 7900HT Sequence Detector (Applied Biosystems). The mean of obtained threshold cycle values (C_t) were analyzed by the comparative C_t method. The respective genes were normalized to human GAPDH, resulting in ΔC_t values. Average ΔC_t values of non-activated cells were deducted from the values of the TNF-α activated cells and the relative mRNA levels were calculated by $2^{-\Delta Ct}$ for the respective genes. Experiments were performed in duplicate with two independently prepared formulations (each time samples were analyzed in duplo).

Effects of rapamycin on signaling events downstream from mTOR were also investigated by anti-phospho-Western blotting. For phospho-Western blotting, HUVEC were seeded at 100,000 cells per well in 6-well plates and allowed to adhere overnight before activation with TNF-α for 4 h at 37 °C and incubation with free rapamycin or liposomal rapamycin formulations at concentration of 10 μM rapamycin for another 4 h at 37 °C. Finally, cells were stimulated by addition of 0.5% insulin for 10 min. Insulin is a known stimulator of the mTOR signaling cascade and activation of the insulin receptor results in phosphorylation of both mTOR (at Ser 2448) and S6-ribosomal protein (at Ser 235/236) kinases (Pellegatta et al., 2006). After washing with cold PBS, the cells were lysed in radioimmuneprecipitation assay (RIPA) buffer, containing phosphatase/kinase inhibitor cocktail (Thermo Fischer Scientific), (120 μl/well), on ice for 30 min and centrifuged at 14,000*g* at 4 °C for 15 min. The obtained supernatants were stored at −20 °C until further evaluation. The protein concentration of the samples was determined by micro-BCA assay. Aliquots corresponding to 15 μg of the protein cell lysate were subjected to SDS-PAGE on 4–12% gradient NuPAGE Novex Bis-Tris mini-gels and electro-transferred onto nitrocellulose membranes via an iBlot Dry Blotting system. Membranes were blocked with 5% BSA in Tris-buffered saline containing 0.1% Tween-20 (TBS-T) for 2 h at room temperature, followed by staining overnight at 4 °C for phospho-mTOR (Ser 2448) and phospho-S6 ribosomal protein (Ser235/236) using rabbit polyclonal antibodies (Cell Signaling Technology, Inc.). β-Actin (Cell Signaling Technology, Inc.) was stained as control. Antibodies were diluted 1:1000 in 5% BSA in TBS-T according to the manufacturer's protocol. After three times washing with TBS-T, membranes were incubated for 1 h at room temperature with goat anti-rabbit peroxidase-conjugated secondary antibody diluted 1:1000 in 5% BSA in TBS-T. Proteins were detected using supersignal west femto chemiluminescent substrate (Thermo Fischer Scientific) and visualized using a Gel Doc imaging system equipped with a XRS camera and Quantity one analysis software (Bio-Rad, Hercules, CA, USA). Densitometric analysis was done using NIH Image J software. Phosphorylation intensity of mTOR and S6 protein of cells exposed to different formulations were normalized versus insulin activated control cells. Experiments were performed in duplicate with two independently prepared formulations.

2.7. Statistical analysis

For the cell-based (*in vitro*) experiments, statistical analysis of the data was performed using Graphpad Prism software (Graphpad software 5.0, San Diego CA, USA), using analysis of variance (ANOVA). Values for the experiments are represented ± SEM, unless stated otherwise. Differences were considered to be significant at values of $P < 0.05$.

3. Results and discussions

3.1. Preparation and characterization of rapamycin-loaded immunoliposomes

PEGylated (immuno)-liposomes loaded with rapamycin were prepared by lipid film hydration and extrusion. Mouse monoclonal anti-human-E-selectin antibodies were conjugated to the maleimidyl-PEG-DSPE anchor after the extrusion steps. The physicochemical properties of the different types of liposomes are given in Table 1. The average liposome size defined by DLS method was 125 nm with a polydispersity index of 0.1. It has been reported that under certain conditions micelles could be an unwanted byproduct in the formulation of liposomes with high-PEG content (Johnsson and Edwards, 2003). In this work the volume-weighted Gaussian distribution (not shown) derived from the DLS analysis showed no micelle formation under the liposomal preparation conditions applied in this work (Weissig et al., 1998).

The prepared liposomes showed a negative zeta-potential of −15 mV, most likely due to the localized negative charges on the phospholipid head groups within the liposomal bilayer (Garbuzenko et al., 2005).

Based on HPLC analysis of destructed liposomes, rapamycin encapsulation efficiency of the liposomes was determined to be approximately 80%, resulting in a formulation with a rapamycin concentration

Table 1
Physicochemical properties of liposomal formulations used in this study.

Samples	Size (nm)*	PDI[a]	Zeta potential (mV)	Total lipid recovery (%)	Rapamycin (mg/ml)	Drug/TL[b] (Mol%)	EE[c] (%)	Ab/Lipo[d]
Control liposomes (non-loaded)	120 ± 9	0.07 ± 0.03	−12.6 ± 3.2	85 ± 2	n/a[e]	n/a	n/a	n/a
Control liposomes (rapamycin loaded)	122 ± 2	0.05 ± 0.02	−11.1 ± 5.0	88 ± 3	0.44 ± 0.01	1.85 ± 0.01	80 ± 3	n/a
Rhodamine-labeled control liposomes (non-loaded)	125 ± 4	0.09 ± 0.08	−17.3 ± 2.0	90 ± 3	n/a	n/a	n/a	n/a
E-selectin targeted loaded liposomes (rapamycin loaded)	134 ± 5	0.13 ± 0.06	−14.1 ± 6.2	86 ± 4	0.45 ± 0.01	1.96 ± 0.04	82 ± 1	6[f]
Rhodamine-labeled E-selectin targeted liposomes (non-loaded)	138 ± 2	0.15 ± 0.07	−15.1 ± 0.9	89 ± 1	n/a	n/a	n/a	6

Data are presented as mean values ± SD of 2–3 preparations.
*Z-average.
[a] Polydispersity index.
[b] Drug/TL mole% determined after liposomal disruption. (The initial Drug/TL mole% prior to liposomal formulation was calculated to be 2).
[c] Encapsulation efficiency = (rapamycin-loaded in lipid bilayer)/(rapamycin added).
[d] Number of attached antibody molecules per liposome.
[e] Not applicable.
[f] The lipid bilayer thickness is corrected for loaded rapamycin, see main text for details.

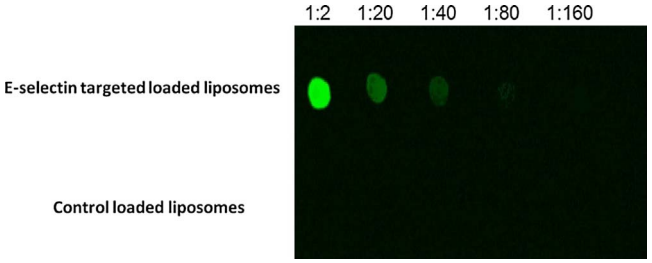

Fig. 2. Dot blot analysis of anti-E-selectin coupling to liposomes. Liposomal stock solutions at indicated dilution ranges were subjected to anti-mouse-IgG immunodetection which demonstrated conjugation of anti-E-selectin mouse-monoclonal antibody to the immunoliposomes..

of 0.45 mg/ml. Dot blot analysis of the liposomes clearly showed the presence of antibody on the surface of targeted liposomes (Fig. 2). From the micro BCA assay the coupling efficiency of the anti-E-selectin to the liposomes was determined to be 77 ± 3% (SD, n = 2), corresponding to 13.4 ± 0.14 (SD, n = 2) μg of anti E-selectin Ab per μmol of total lipid. Combining formula (1) given in Section 2.3 with the literature values for specific lipid volume (V_{Ls}) of 1.25 $nm^3$and liposome bilayer thickness (d_{bl}) of 3.7 nm (Enoch and Strittmatter, 1979), plus the molecular weight of anti E-selectin Ab (approximately 150 kDa), results in a calculated average of 5.6 Ab molecules coupled per liposome (i.e. 6 Ab molecules/liposome). However, intercalation of the loaded hydrophobic drug compound (i.e. rapamycin) into the hydrocarbon chain region in the lipid bilayer could lead to variations in bilayer thickness, due to changes in the molecular conformation of the intercalated (drug) compound (Sun et al., 2008). This effect has previously been reported to result in a 10% increase in liposome bilayer thickness (d_{bl}) of DPPC domains loaded with the drug Atorvastatin (Redondo-Morata et al., 2016). Recalculation of the antibody density assumuing a similar increase in liposome bilayer thikness (i.e. 10% increase in d_{bl}) yielded an average of 5.9 Ab molecules/liposome.

3.2. Cellular handling of E-selectin targeted liposomes by activated endothelial cells

The ability of anti-E-selectin targeted liposomes in binding and uptake by TNF-α activated endothelial cells was studied by fluorescence microscopy and flow cytometry measurements, respectively. The interaction of immunoliposomes with activated HUVEC was visualized by means of fluorescence microscopy (Fig. 3). Anti-E-selectin immunoliposomes were effectively internalized by the activated endothelial cells, while control liposomes showed significantly less internalization (Fig. 4).

3.3. Pharmacological activity of rapamycin-loaded liposomes

3.3.1. Cell viability assessment

TNF-α activated HUVEC treated with different concentrations of rapamycin for 48 h did not show reduced viability at concentrations of rapamycin up to 25 μM. A sharp decrease in cell viability was found at a rapamycin concentration of 50 μM (Fig. 5). Combining this data with results from previous studies (Salas-Prato et al., 1996; Yang et al., 2015), 10 μM rapamycin was chosen as a non-toxic concentration at which anti-inflammatory and other pharmacological effects of targeted liposomal rapamycin formulations can be evaluated.

3.3.2. Effects of rapamycin liposomes in scratch wound assay

The mTOR signaling cascade controls a wide range of cellular responses, including cell migration (Berven and Crouch, 2004). To investigate the pharmacological activity of rapamycin-loaded liposomal formulations the

migration of endothelial cells was studied in a scratch wound assay. Semi-quantitative analysis of the scratch wound area revealed that TNF-α treated endothelial cells (control) repopulated the cell-free area for more than 90% in 16 h. Treatment with free rapamycin reduced the closure of the scratch area to 50% in 16 h (supplemental material Fig. S1 and Fig. 6). Non-targeted liposomes showed a slight 20 reduction of the scratch wound area closure compared to the control, which was most likely caused by unspecific uptake of the liposomes by the cells within the set exposure time. Importantly, E-selectin targeted liposomes loaded with rapamycin showed significantly enhanced inhibition of cell migration, with a reduction of up to 60% compared to untreated endothelial cells. One way to explain the mechanisms behind the inhibition of cell migration and cell motility induced by cytokines such as TNF-α

is that inhibition of mTOR also blocks the action of vascular endothelial cell growth factor A (VEGF), which is a critical regulator of angiogenesis and endothelial cell migration through both inhibition of VEGF synthesis and its signal transduction (Guba et al., 2002; Del Bufalo et al., 2006). Another way to explain the phenomena is that rapamycin has an inhibitory effect on mTORc1 by preventing the interaction of mTOR with the raptor protein scaffold (Arsham and Neufeld, 2006).

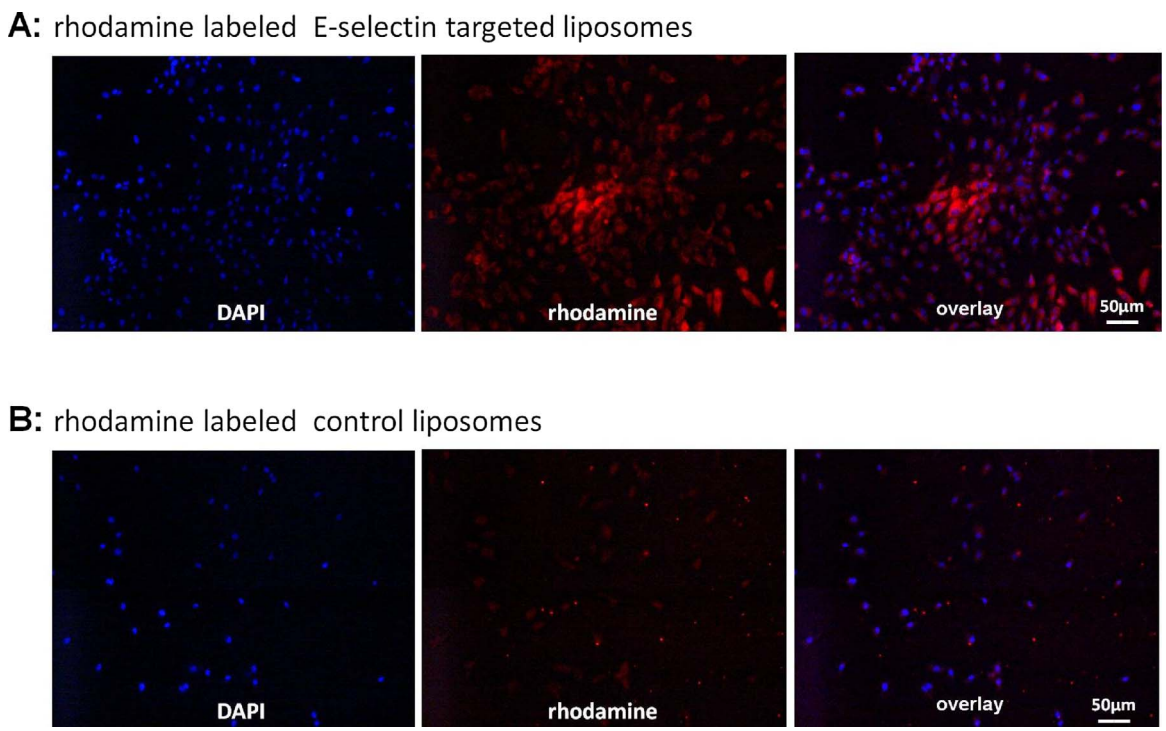

Fig. 3. Wide-field fluorescence microscopy pictures of TNF-α activated HUVEC incubated (4 h) with rhodamine labeled liposomes. **(A):** rhodamine labeled E-selectin targeted liposomes; **(B):** rhodamine labeled control liposomes. Objective lens magnification of 20×. Rhodamine is depicted as red, DAPI (nuclear staining) as blue. Scale bars in the figures represent 50 µm. (For interpretation of the references to colour in this figure legend, the reader is referred to the web version of this article.)

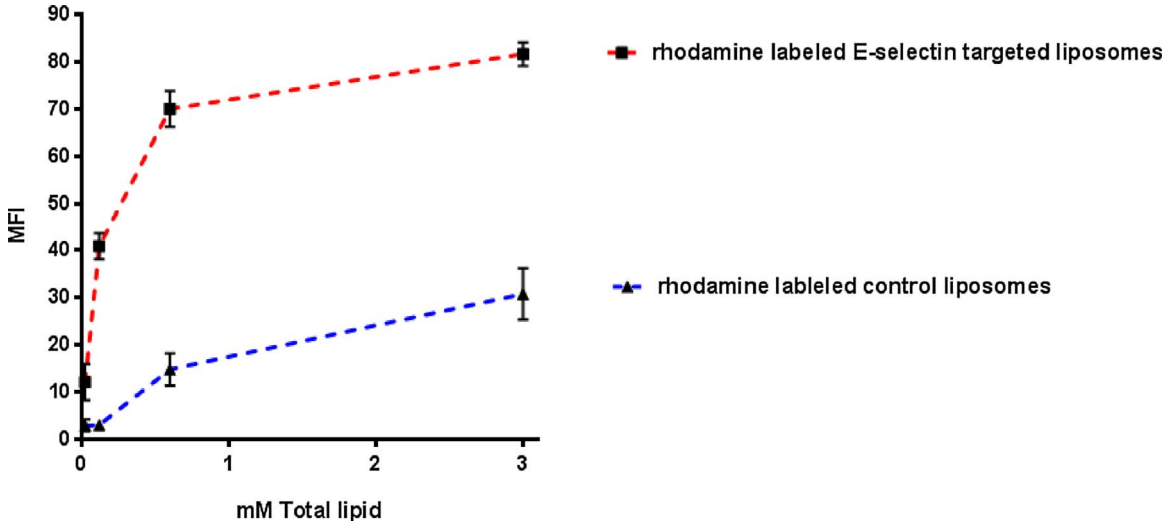

Fig. 4. Internalization of E-selectin targeted liposomes by activated endothelial cells. Mean Fluorescence Intensity (MFI) of cells incubated with rhodamine labeled E-selectin targeted liposomes (■) and rhodamine labeled control liposomes (▲) after 3 h incubation at 37 °C. Cells were treated with an acid wash (pH: 3.0) after incubations to remove surface bound liposomes. Data are presented as mean ± SEM of three experiments using the same formulation.

3.3.3. Effects of rapamycin formulations on proliferation of activated endothelial cells

Both endothelial migration and proliferation can contribute to closure of the scratch wounds, as discussed in the previous paragraph. Although we studied the scratch wound healing at incubation times shorter than the doubling time of HUVEC (approximately 48 h) overnight repopulation of the scratch wound area cannot be fully attributed to endothelial cell migration only. We therefore studied the potential inhibitory effects on endothelial cell proliferation in two different setups, using either prolonged exposure for a period of 48 h or short-term exposure for 4 h followed by a 44 h recovery (i.e. treatment-free) period. The latter experimental conditions mimic *in vivo* drug exposure, in which drug peak levels are alternated with drug-free periods. To investigate the correlation between absorption value (BrdU incorporation) and number of proliferating cells, a calibration curve was made out of serial dilutions of HUVEC per well. In this way, the absolute absorbance values obtained for control cells and each of the treatments could be converted to the number of proliferating cells per well (Fig. 7A). In the short term exposure study (Fig. 7B) neither free rapamycin, nor the control loaded liposomal formulation of rapamycin significantly affected endothelial cell proliferation in the studied dose range. Only the highest concentration of E-selectin targeted rapamycin-loaded liposomes (25 µM) showed slight reduction (~10%) in endothelial cell proliferation from average 5722 cells/well (control) down

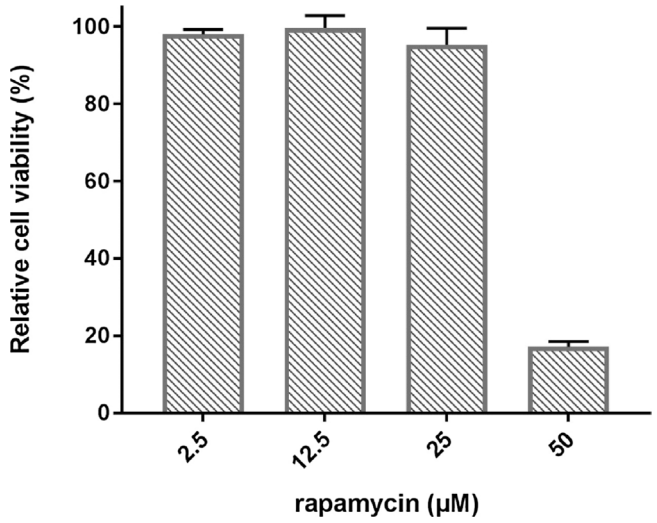

Fig. 5. MTS cell viability assay on TNF-α activated HUVEC. Cells were exposed to solutions containing different concentrations of rapamycin for 48 h. Data are normalized compared to control (non-treated) cells. Results are presented as mean ± SEM of three experiments.

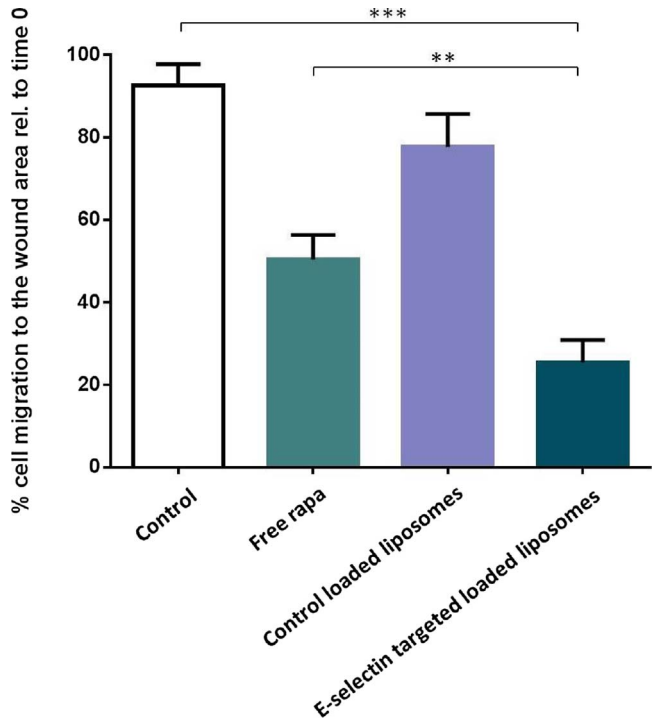

Fig. 6. Effect of rapamycin-loaded liposomes on migration of TNF-α activated endothelial cells. Repopulation of endothelial cells in a scratch wound was investigated with TNF-α activated HUVEC that had been pre-incubated with rapamycin formulations at 10 μM for 12 h. Data have been expressed as semi-quantitative analysis of closure of the scratch wound area, as calculated from the images taken at t = 0 h and t = 16 h (see supplemental material for images). Data are plotted as mean values ± SEM of three experiments with the same formulations; **p < 0.01, ***p < 0.001 compared to free rapamycin and control.

to 5081 (cells/well). After long-term exposure of 48 h (Fig. 7C), both free rapamycin and E-selectin targeted liposomes loaded with rapamycin inhibited endothelial cell proliferation, while control loaded liposomes showed less anti- proliferative activity. The contribution of E-selectin directed uptake of rapamycin-loaded liposomes was most prominently observed at 1 and 5 μM concentrations, which highlights the added value of targeted liposomes for intracellular delivery of rapamycin. At high concentrations of rapamycin (25 μM), passive uptake of free rapamycin and receptor-mediated uptake of rapamycin-loaded immunoliposomes resulted in similar effects of the delivered drug within the target cells, which can be attributed to saturation of the E-selectin uptake pathway and to overall saturation of the mTOR inhibition by rapamycin under those conditions. Lastly, control liposomes did not show any effect on cell proliferation in the short-term assay and only showed activity after continuous exposure, which can be explained by the presence of some non-specific uptake of the liposomes upon continuous incubation.

The results obtained from this experiment correlate well with the previously discussed inhibiting effect of rapamycin on cell migration and motility. It can be concluded that within the 16 h time frame at concentration of 10 μM, the rapamycin inhibiting effect on the repopulation of the scratch wound area is not entirely due to its effect on cell motility and migration, but can also be attributed to its anti-proliferative effect.

3.3.4. *Effects of rapamycin liposomes on gene expression*

Real-time q-PCR analysis was used to examine whether rapamycin and its liposomal formulations affect mRNA expression of proteins related to inflammation under TNF-α activated and/or non-activated conditions (Fig. 8). In total 6 genes were studied, including: inflammation induced adhesion molecules (VCAM-1 and E-selectin); angiogenesis mediators (TIE2 receptor and VEGF); fibrosis cytokine (TGF-α) and mTOR itself. First, the effect of TNF-α on the gene expression of the selected genes was evaluated. The activated cells showed a strong (> 100 fold) increase in gene expression of both VCAM-1 and E-selectin (Fig. 8A and B). Expression of adhesion molecules, especially E-selectin, plays a main role in this study as specific binding of the immunoliposomes to E-selectin mediates liposome uptake. The cell binding assays discussed in Section 3.2 (see also Fig. 3) showed that E-selectin expression is already elevated at t = 4 h (i.e. the time point for adding the liposomal formulations to the cells). The results on the gene expression of adhesion molecules indicate that their expression is enhanced in presence of TNF-α even at t = 24 h. In general, these findings are consistent with previous studies in which it was shown that exposure to TNF-α either after 4 or 24 h induces the expression of E-selectin and VCAM-1 mainly via activation of NF-αB pathway (Wagener et al., 1997; Rahman et al., 1998).

Upon activation of the cells with TNF-α, a 4.4 and 5.6 fold increase in gene expression of angiogenesis mediators was observed, compared to resting cells, for the TIE2 angiopoietin receptor and the VEGF ligand respectively (Fig. 8C and D). However, the precise role of TNF-α in angiogenesis has been a subject of debate in scientific literature (Sainson et al., 2008). Several *in vitro* studies have shown that TNF-α can be either proangiogenic or antiangiogenic, depending mainly on cell environmental factors (Sainson et al., 2008). With the experimental conditions used in this work, we demonstrated that TNF-α induced gene expression of both the TIE2 receptor and the VEGF ligand. These findings are in good agreement with previous studies that also reported that TNF-α induced these above mentioned gene expressions (TIE2 and VEGF), both of which are reported to be mediated through the NF-αB pathway (DeBusk et al., 2003; Chen et al., 2004; Nagineni et al., 2012; Yuan et al., 2012).

TGF-α is a pleiotropic cytokine which has either inflammatory or anti-inflammatory activities, depending on the cellular environment. In this study, we could not detect changes in TGF-α gene expression upon cell activation with TNF-α (Fig. 8E). Using different cell types, a study by Chen and coworkers reported that TNF-α expression induced TGF-α secretion in macrophages and vice versa (Chen et al., 2008), while another study by Sullivan and coworkers demonstrated that TNF-α plays significant role in regulating TGF-α in lung fibroblasts through AP-1 activation *in vitro* (Sullivan et al., 2009). However, under the experimental conditions we could not detect any change in TGF-α gene expression between the cells activated with TNF-α and the non-activated resting cells.

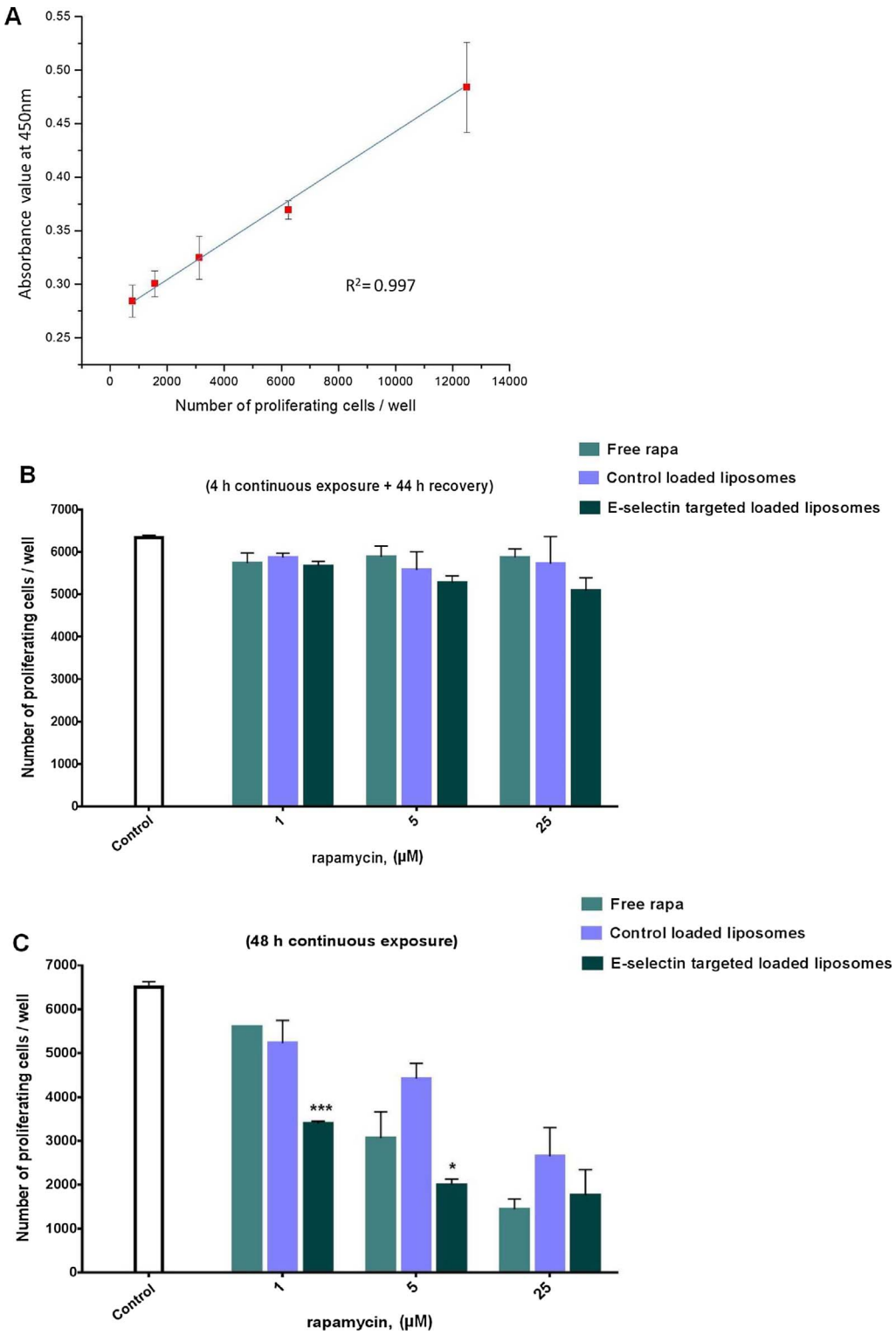

Fig. 7. Cell proliferation was determined in TNF-α activated HUVEC by BrdU-incorporation after 48 h of total incubation period. **(A):** Effect of proliferating cell number on absorbance at 450 nm, measured using BrdU incorporation assay. **(B):** Cells were exposed for 4 h to rapamycin formulations followed by recovery period of 44 h in fresh medium. **(C):** Cells were exposed for 48 h to rapamycin formulations continuously. Data are plotted as mean values ± SEM of three experiments with the same formulations; *p < 0.05, ***p < 0.001 compared to free rapa treatment.

The results obtained in this work show an approximately 2-fold increase in mTOR gene expression for the TNF-α activated cells compared to the resting cells (Fig. 8F). This is consistent with previous studies which showed that TNF-α up-regulates mTOR gene expression by activation of the NF-αB pathway (Dan et al., 2008; Karonitsch et al., 2015).

When introduced to TNF-α activated cells, both free rapamycin and immunoliposomes loaded with rapamycin significantly reduced the gene expressions of VCAM-1, E-selectin, VEGF and TIE2, as shown in Fig. 8A–D. However, no effect was detected for mTOR and TGF-α gene expressions (Fig. 8E, F). Control (i.e. non-targeted) liposomes loaded with rapamycin showed less effect on the overall gene expression as compared to their (targeted) counterparts. Taken together, the data suggest that the liposomal formulation that allows for targeted rapamycin delivery into inflammation activated endothelial cells, mediates on average 50% downregulation of the target genes (i.e. VCAM-1, E-selectin, VEGF and TIE2) compared to TNF-α activated (control +) cells. Free rapamycin also caused a significant

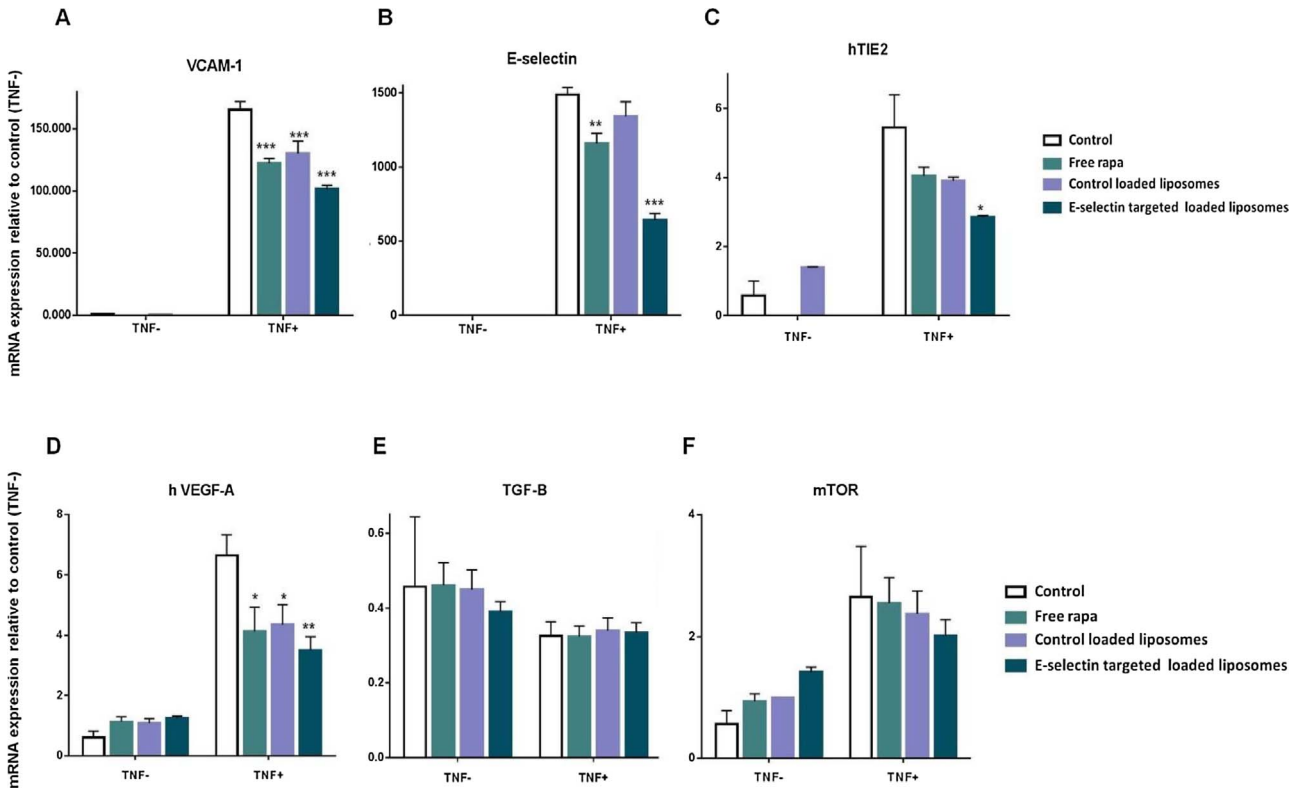

Fig. 8. TNF-α activated and non-activated HUVEC were treated with rapamycin and its liposomal formulations for 24 h. **(A)** VCAM-1, **(B)** E-selectin, **(C)** hTIE2, **(D)** h VEGF-A, **(E)** TGF-α **(F)** mTOR gene expressions determined by q-PCR analyses. Total mRNA input was corrected for the housekeeping gene hGAPDH. Quantitative change in expression was calculated relative to resting cells (TNF-). Data are plotted as mean values ± SEM of two independent experiments; *p < 0.05, **p < 0.01, ***p < 0.001 compared to TNF-α activated control cells (TNF +).

decrease in the expression of these same genes compared to TNF-α activated (control +) cells, which confirms that the drug itself is responsible for inducing the reported effects in HUVEC. Encapsulation of rapamycin in liposomes is intended to improve selectivity versus a specific cell type (in present study: inflammation activated endothelium), thus avoiding other cell types. Hence, the comparison between targeted liposomes and control liposomes loaded with rapamycin better reflects the improvement obtained by targeted delivery via E-selectin. Our results demonstrate that the final formulation retains its efficacy (at equal levels to free rapamycin) while we also demonstrate the importance of E-selectin mediated active uptake which is specific for endothelial cells. Targeted liposomes were (at least) 15% more effective in inhibiting gene expression than free rapamycin. When comparing their impact on the expression of E-selectin (Fig. 8B), the difference between targeted liposomes loaded with rapamycin and free rapamycin is even more pronounced. Similar results regarding the effectiveness of the targeted liposomes are also observed in cell migration and proliferation assays. Most likely, the active delivery of rapamycin by the targeted liposomes resulted in the highest intracellular concentrations within the designated time period.

3.3.5. *Effects of rapamycin liposomes on mTOR signaling cascade*

To induce E-selectin over-expression on the surface of the HUVEC, the cells were first exposed to TNF-α for 4 h. As shown previously, this step is essential for active binding and uptake of E-selectin targeted liposomes, while TNF-α is also one of the inflammatory cytokines that affects cell signaling pathways, such as activation of mTOR in HUVEC (Glantschnig et al., 2001). Insulin is known to strongly modulate downstream effectors in the mTOR pathway (Pellegatta et al., 2006). For more details on the effects of insulin on the mTOR pathway, the reader is referred to the works of Garami et al. and Nave et al. (Garami et al., 2003; Nave et al., 1999). Therefore, several experiments were performed to determine whether incubating HUVEC with solely TNF-α or with a combination of TNF-α and insulin would have an effect on the phosphorylation of Ser $^{235/236}$ of the S6 ribosomal protein and Ser^{2448} of mTOR. Activation with only TNF-α induced a 72% and 85% increase in the degree of phosphorylation of mTOR and S6 proteins respectively, compared to resting cells (control). Exposure of the cells to insulin in the presence of TNF-α resulted in an increase versus control of 146% and 120% in phosphorylation of mTOR and S6 proteins respectively (Fig. 9A–B). While previous studies have reported an increase in phosphorylation of mTOR and S6 proteins through a PI3kinase-Akt dependent pathway upon exposure to insulin, such an effect has not yet been reported in the presence of TNF-α (Scott et al., 1998; Reynolds et al., 2002; Garami et al., 2003).

Both free rapamycin and E-selectin targeted liposomes loaded with rapamycin inhibited phosphorylation of mTOR and S6 after a 4 h incubation at a concentration of 10 μM of rapamycin, while control (i.e. non-targeted) liposomes loaded with rapamycin showed almost no inhibitory effect (Fig. 10A and B). These findings are in good agreement with our results from the cell migration, proliferation and gene expression assays, in which E-selectin targeted liposomes loaded with rapamycin showed a more pronounced inhibiting effect than its non-targeted counterparts. It should be noted that the conditions in this experiment differed slightly from the cell migration, proliferation and gene expression assays described in earlier paragraphs, because insulin was applied as an additional stimulating factor for the short-lived activation of the mTOR pathway upon treatment with rapamycin.

4. Conclusion

Free rapamycin is a potent and efficacious drug in the treatment of inflammatory disorders; its use is however associated with side effects. The present approach involving its encapsulation in immunoliposomes

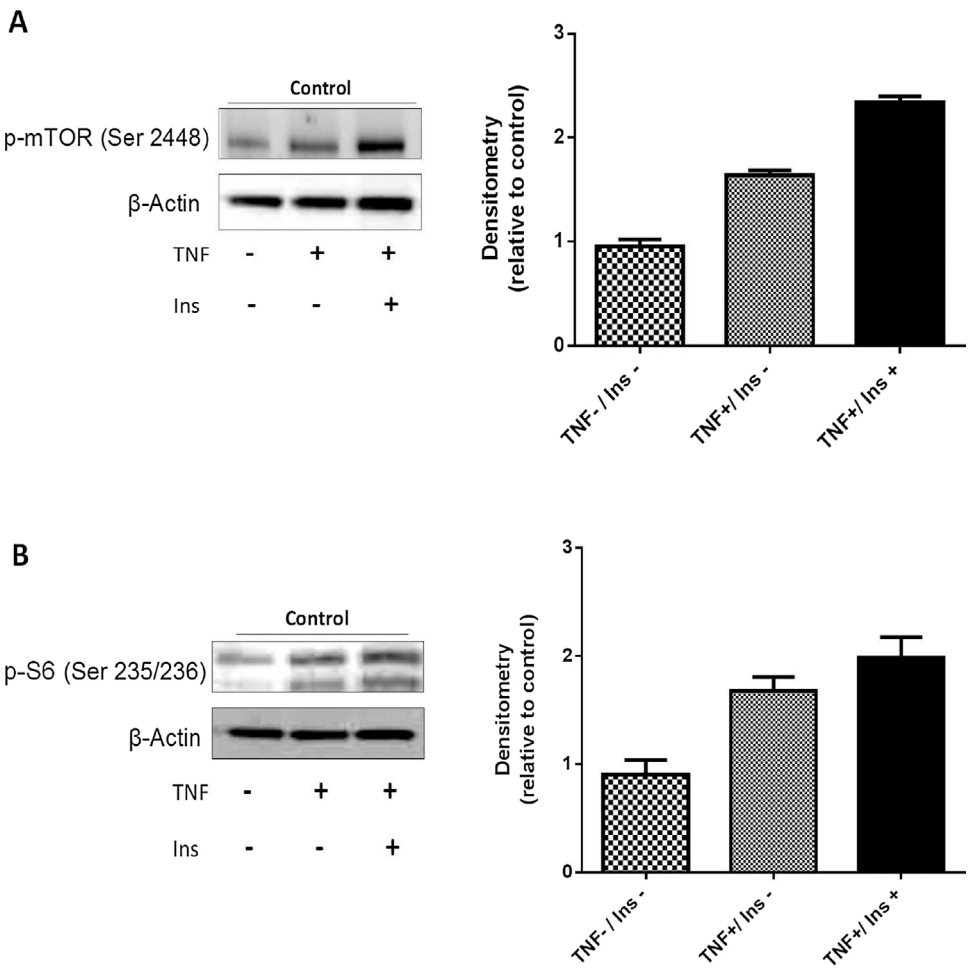

Fig. 9. Effect of stimulation with TNF-α and combined stimulation with TNF-α and insulin on phosphorylation of mTOR **(A)** and S6 ribosomal protein **(B)** in HUVEC. Data are plotted as mean values ± SEM of two experiments with two separately prepared formulations.

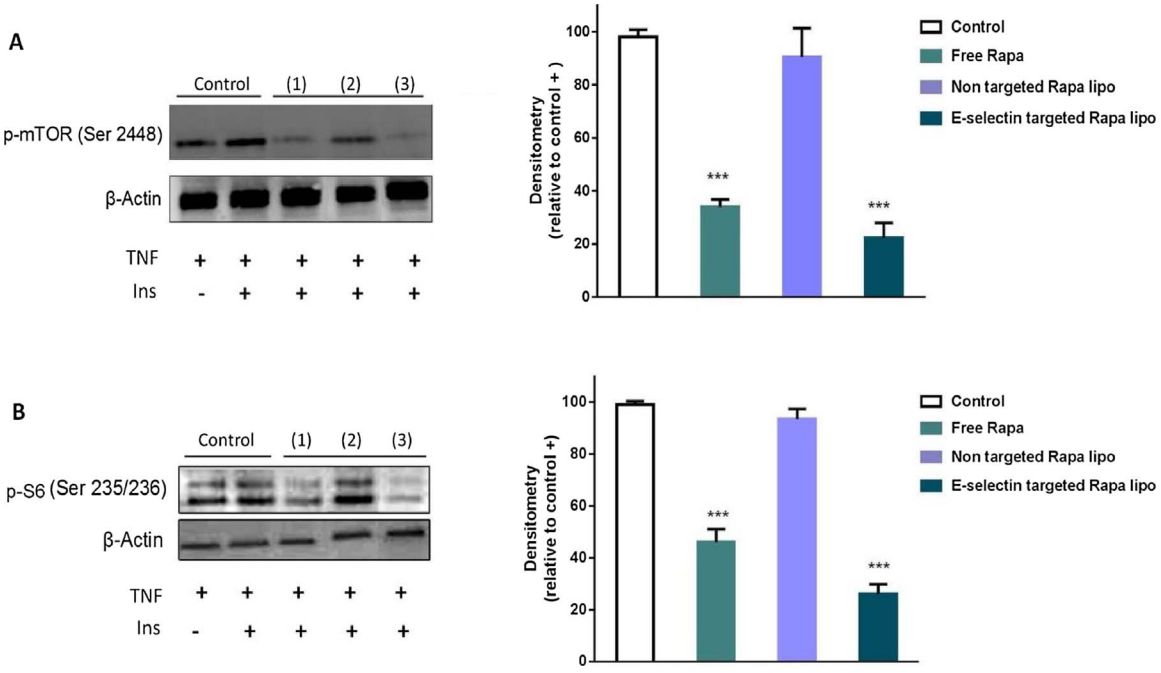

Fig. 10. Effect of rapamycin and its liposomal formulations (equivalent to 10 μM rapamycin) on phosphorylation of mTOR **(A)** and S6 ribosomal protein (lower band) **(B)** in HUVEC. **(1)** represents free rapamycin; **(2)** control loaded liposomes and **(3)** E-selectin targeted loaded liposomes. Data are plotted as mean values ± SEM of two experiments with two separately prepared formulations; ***$p < 0.001$ compared to control+.

will provide for a more selective activity of the drug targeted to a specific cell type. Anti-E-selectin immunoliposomes were shown to be attractive nanocarrier systems for targeted delivery of rapamycin to TNF-α activated endothelial cells. Further studies to evaluate *in vivo* efficacy of rapamycin loaded immunoliposomes are necessary to fully address their value for anti-inflammatory therapy.

Conflict of interest

The authors declare no conflict of interest.

Acknowledgments

This work has been supported by NanoNextNL, a micro and nanotechnology consortium of the government of The Netherlands and 130 partners (project 03D.07). The authors would like to thank Mies van Steenbergen (Utrecht University) for his expert technical assistance.

Appendix A. Supplementary data

Supplementary data associated with this article can be found, in the online version, at https://doi.org/10.1016/j.ijpharm.2017.10.027.

References

Adrian, J.E., Scherphof, G.L., Meijer, D.K., van Loenen-Weemaes, A.M., Reker-Smit, C., Terpstra, P., Poelstra, K., 2007. A novel lipid-based drug carrier targeted to the non-parenchymal cells, including hepatic stellate cells, in the fibrotic livers of bile duct ligated rats. Biochim. Biophys. Acta 1768 (6), 1430–1439.
Arsham, A.M., Neufeld, T.P., 2006. Thinking globally and acting locally with TOR. Curr. Opin. Cell Biol. 18 (6), 589–597.
Berven, L.A., Crouch, M.F., 2004. Role of the p70(S6K) pathway in regulating the actin cytoskeleton and cell migration. Exp. Cell Res. 296, 183–195.
Bonegio, R.G., Wang, Z., Valeri, C.R., Andry, C., Salant, D.J., Lieberthal, W., 2005. Rapamycin ameliorates proteinuria-associated tubulointerstitial inflammation and fibrosis in experimental membranous nephropathy. J. Am. Soc. Nephrol. 16, 2063–2072.
Cejka, D., Niederreiter, B., Sieghart, W., Fuereder, T., Zwerina, J., Schett, G., 2010. Mammalian target of rapamycin signaling is crucial for joint destruction in experimental arthritis and is activated in osteoclasts from patients with rheumatoid arthritis. Arthritis Rheum. 62 (8), 2294–2302.
Chen, J.X., Chen, Y., DeBusk, L., Lin, W., Lin, P.C., 2004. Dual functional roles of Tie-2/angiopoietin in TNF-a-mediated angiogenesis. Am. J. Physiol. Heart Circ. Physiol. 287, 187–195.
Chen, Y., Liu, F.Q., Liu, Y., Lui, V.C., Lamb, J.R., Tam, P.K., 2008. LPS-induced up-regulation of TGF-beta receptor 1 is associated with TNF-alpha expression in human monocyte-derived macrophages. J. Leukoc. Biol. 83 (5), 1165–1173.
Chen, Y.C., Lin, Y.F., Hsiue, G.H., 2013. Rapamycin encapsulated in dual-responsive micelles for cancer therapy. Biomaterials 34, 1115–1127.
Cook-Mills, J.M., Deem, T.L., 2005. Active participation of endothelial cells in inflammation. J. Leukoc. Biol. 77 (4), 487–495.
Dan, H.C., Cooper, M.J., Cogswell, P.C., Duncan, J.A., Ting, J.P., Baldwin, A.S., 2008. Akt-dependent regulation of NF-{kappa} B is controlled by mTOR and Raptor in association with IKK. Genes Dev. 22, 1490–1500.
DeBusk, L.M., Nishishita, T., Chen, J., Thomas, J.W., Lin, P.C., 2003. Tie2 receptor tyrosine kinase, a major mediator of tumor necrosis factor alpha-induced angiogenesis in rheumatoid arthritis. Arthritis Rheum. 48 (9), 2461–2471.
Del Bufalo, D., Trisciuoglio, D., Desideri, M., Cognetti, F., Zupi, G., Milella, M., 2006. Antiangiogenic potential of the Mammalian target of rapamycin inhibitor temsirolimus. Cancer Res. 66 (11), 5549–5554.
Eloy, J.O., Petrilli, R., Topan, J.F., Antonio, H.M., et al., 2016. Co-loaded paclitaxel/rapamycin liposomes Development, characterization and in vitro and in vivo evaluation for breast cancer therapy. Colloids Surf. B Biointerfaces 41, 74–82.
Enoch, H.G., Strittmatter, P., 1979. Formation and properties of 1000-Å-diameter: single-bilayer phospholipid vesicles. Proc. Natl. Acad. Sci. 76, 145–149.
Everts, M., Kok, R.J., Asgeirsdóttir, S.A., Vestweber, D., Meijer, D.K., Storm, G., Molema, G., 2003. In vitro cellular handling and in vivo targeting of E-selectin-directed immunoconjugates and immunoliposomes used for drug delivery to inflamed endothelium. Pharm. Res. 20 (1), 64–72.
Garami, A., Zwartkruis, F.J., Nobukuni, T., Joaquin, M., Roccio, M., Stocker, H., Kozma, S.C., Hafen, E., Bos, J.L., Thomas, G., 2003. Insulin activation of Rheb, a mediator of mTOR/S6K/4E-BP signaling, is inhibited by TSC1 and 2. Mol. Cell 11, 1457–1466.
Garbuzenko, O., Zalipsky, S., Qazen, M., Barenholz, Y., 2005. Electrostatic of PEGylated micelles and liposomes containing charged and neutral lipopolymers. Langmuir 21 (6), 2560–2568.
Glantschnig, H., Fisher, J.E., Wesolowski, G., Rodan, G.A., Reszka, A.A., 2001. M-CSF, TNF, and RANK ligand promote osteoclast survival by signaling through mTOR/S6 kinase. Cell Death Differ. 10, 1165–1177.
Guba, M., Steinbauer, M., Koehl, G., Flegel, S., Hornung, M., et al., 2002. Rapamycin inhibits primary and metastatic tumor growth by antiangiogenesis: involvement of vascular endothelial growth factor. Nat. Med. 8 (2), 128–135.
Hu, X., Chen, D., Zhang, J., Liu, Z., Wu, W., et al., 2012. Sirolimus solid self-micro-emulsifying pellets Formulation development, characterization and bioavailability evaluation. Int. J. Pharm. 438, 123–133.
Jacinto, E., Schmidt, A., Lin, S., Rüegg, M.A., Hall, A., Hall, M.N., 2004. Mammalian TOR complex 2 controls the actin cytoskeleton and is rapamycin insensitive. Nat. Cell Biol. 6, 1122–1128.
Johnsson, M., Edwards, K., 2003. Liposomes, disks, and spherical micelles: aggregate structure in mixtures of gel phase phosphatidylcholines and poly(ethylene glycol)-phospholipids. Biophys. J. 85 (6), 3839–3847.
Karonitsch, T., Herdy, B., Kandasamy, K., Niederreiter, B., et al., 2015. AB0075 MTOR: an unexpected role on the TNF-Regulated MRNA transcriptome in rheumatoid fibroblast-Like synoviocytes. Ann. Rheum. Dis. 74, 915–916.
Kim, D.H., Ali, S.M., King, J.E., Latek, R.R., Erdjument-Bromage, H., Tempst, P., Sabatini, D.M., 2002. mTOR interacts with raptor to form a nutrient-sensitive complex that signals to the cell growth machinery. Cell 110, 163–175.
Koning, G.A., Wauben, M.H., Kok, R.J., Mastrobattista, E., Molema, G., ten Hagen, T.L., Storm, G., 2006. Targeting of angiogenic endothelial cells at sites of inflammation by dexamethasone phosphate-containing RGD peptide liposomes inhibits experimental arthritis. Arthritis Rheum. 54 (4), 1198–1208.
Li, D., Wang, C., Yao, Y., Chen, L., Liu, G., Zhang, R., Liu, Q., Shi, F.D., Hao, J., 2016. mTORC1 pathway disruption ameliorates brain inflammation following stroke via a shift in microglia phenotype from M1 type to M2 type. FASEB J. 30 (10), 3388–3399.
Lieberthal, W., Levine, J.S., 2009. The role of the mammalian target of rapamycin (mTOR) in renal disease. J. Am. Soc. Nephrol. 20, 2493–2502.
Lieberthal, W., Levine, J.S., 2012. Mammalian target of rapamycin and the kidney II. Pathophysiology and therapeutic implications. Am. J. Physiol. Renal Physiol. 15, 180–191.
Martini, F.H., et al., 2012. Fundamentals of Anatomy & Physiology. Pearson education Inc.
Muller, W.A., 2003. Leukocyte-endothelial-cell interactions in leukocyte transmigration and the inflammatory response. Trends Immunol. 24, 327–334.
Nagineni, C.N., William, A., Detrick, B., Hooks, J.J., 2012. Regulation of VEGF expression in human retinal cells by cytokines: implications for the role of inflammation in age-related macular degeneration. J. Cell. Physiol. 227 (1), 116–126.
Nave, B.T., Ouwens, M., Withers, D.J., Alessi, D.R., Shepherd, P.R., 1999. Mammalian target of rapamycin is a direct target for protein kinase B: identification of a convergence point for opposing effects of insulin and amino-acid deficiency on protein translation. Biochem. J 344, 427–431.
Panés, J., Perry, M., Granger, D.N., 1999. Leukocyte-endothelial cell adhesion: avenues for therapeutic intervention. Br. J. Pharmacol. 126, 537–550.
Pellegatta, F., Catapano, A.L., Luzi, L., Terruzzi, I., 2006. In human endothelial cells amino acids inhibit insulin-induced Akt and ERK1/2 phosphorylation by an mTOR-dependent mechanism. J. Cardiovasc. Pharmacol. 47 (5), 643–649.
Rahman, A., Kefer, J., Bando, M., Niles, W.D., Malik, A.B., 1998. E-selectin Expression in Human Endothelial Cells by TNF-a-induced Oxidant Generation and NF-kB Activation. The American Physiological Society.
Redondo-Morata, L., Lea Sanford, R., Andersen, O.S., Scheuring, S., 2016. Effect of statins on the nano-mechanical properties of supported lipid bilayers. Biophys. Soc. 111 (2), 363–372.
Reynolds, T.H., Bodine, S.C., Lawrence Jr, J.C., 2002. Control of Ser2448 phosphorylation in the mammalian target of rapamycin by insulin and skeletal muscle load. J. Biol. Chem. 277 (20), 17657–17662.
Rouser, G., Fkeischer, S., Yamamoto, A., 1970. Two dimensional thin layer chromatographic separation of polar lipids and determination of phospholipids by phosphorus analysis of spots. Lipids 5, 494–496.
Sainson, R.C., Johnston, D.A., Chu, H.C., Holderfield, M.T., et al., 2008. TNF primes endothelial cells for angiogenic sprouting by inducing a tip cell phenotype. Blood 111, 4997–5007.
Salas-Prato, M., Mehdi, A.Z., Duperré, J., Thompson, P., Brazeau, P., 1996. Inhibition by rapamycin of PDGF- and bFGF-induced human tenon fibroblast proliferation in vitro. J. Glaucoma 5 (1), 54–59.
Sarbassov, D.D., Kim, D.H., Guertin, D.A., et al., 2004. Rictor, a novel binding partner of mTOR, defines a rapamycin-insensitive and raptor-independent pathway that regulates the cytoskeleton. Curr. Biol. 14, 1296–1302.
Scott, P.H., Brunn, G.J., Kohn, A.D., Roth, R.A., Lawrence Jr., J.C., 1998. Evidence of insulin-stimulated phosphorylation and activation of the mammalian target of rapamycin mediated by a protein kinase B signaling pathway. Proc. Natl. Acad. Sci. 95 (13), 7772–7777.
Shah, M., Janga, S.R., Shi, P., Dhandhukia, J., Liu, S., et al., 2013. A rapamycin-binding protein polymer nanoparticle shows potent therapeutic activity in suppressing autoimmune dacryoadenitis in a mouse model of Sjogren's syndrome. J. Control. Release 171, 269–279.
Simamora, P., Yalkowsky, S.H., 2001. Solubilization of rapamycin. Int. J. Pharm. 213, 25–29.
Sullivan, D.E., Nguyen, H., Abboud, E., Brody, A.R., 2009. TNF-alpha induces TGF-beta1 expression in lung fibroblasts at the transcriptional level via AP-1 activation. J. Cell. Mol. Med. 13 (8), 1866–1876.
Sun, Y., Lee, C.C., Hung, W.C., Chen, F.Y., Lee, M.T., Huang, H.W., 2008. The bound states of amphipathic drugs in lipid bilayers: study of Curcumin. Biophys. J. 95, 2318–2324.
Wagener, F.A., Feldman, E., de Witte, T., Abraham, N.G., 1997. Heme induces the expression of adhesion molecules ICAM-1, VCAM-1, and E selectin in vascular endothelial cells. Proc. Soc. Exp. Biol. Med. 216 (3), 456–463.

Weichhart, T., Hengstschläger, M., Linke, M., 2015. Regulation of innate immune cell function by mTOR. Nat. Rev. Immunol. 15, 599–614.
Weissig, V., Whiteman, K.R., Torchilin, V.P., 1998. Accumulation of protein-Loaded long-circulating micelles and liposomes in subcutaneous lewis lung carcinoma in mice. Pharm. Res. 15 (10), 1552–1556.
Woo, H.N., Ju, E.J., Jung, J., Kang, H.W., Lee, S.W., et al., 2012. Preclinical evaluation of injectable sirolimus formulated with polymeric nanoparticle for cancer therapy. Int. J. Nanomed. 7, 2197–2208.
Wu, M.J., Wen, M.C., Chiu, Y.T., Chiou, Y.Y., Shu, K.H., Tang, M.J., 2006. Rapamycin attenuates unilateral ureteral obstruction-induced renal fibrosis. Kidney Int. 69, 2029–2036.
Wullschleger, S., Loewith, R., Hall, M.N., 2006. TOR signaling in growth and metabolism. Cell 124, 471–484.
Xie, L., Sun, F., Wang, J., Mao, X., Xie, L., Yang, S.H., Su, D.M., et al., 2014. mTOR signaling inhibition modulates macrophage/microglia-mediated neuroinflammation and secondary injury via regulatory T cells after focal ischemia. J. Immunol. 192 (12), 6009–6019.
Yang, P., Zhao, Y., Zhao, L., Yuan, J., et al., 2015. Paradoxical effect of rapamycin on inflammatory stress-induced insulin resistance in vitro and in vivo. Sci. Rep. 5, 149–159.
Yuan, J., Fang, W., Lin, A., Ni, Z., Qian, J., 2012. Angiopoietin-2/Tie2 signaling involved in TNF-alpha induced peritoneal angiogenesis. Int. J. Artif. Organs 35 (9), 655–662.